

Summary of 2022 01 03 Earthquake Event

1 - Introduction

A local magnitude (M_L) 6.0 event occurred at 17:46 on January 3 this year (2022). The Central Weather Bureau (CWB) of Taiwan announced that the real-time solution for the epicenter located it at 24.02 N / 122.18 E and the focal depth at 19.4 km (Fig. 1). Seismic intensities of 4 were observed in Taipei, New Taipei, and Yilan regions, but didn't cause severe damage. The Taiwan Early Seismic Loss Estimation module of the Taiwan Earthquake Loss Estimation System (TELES) developed by the National Center for Research on Earthquake Engineering (NCREE) can perform seismic loss estimation and send text messages (Fig. 2) within two minutes of receiving the earthquake report from the CWB via email. The estimation results show that no casualties were caused in this seismic event.

occurred historically in surrounding regions, including the events that occurred on June 5, 1920 and March 31, 2002. The Taiwan Earthquake Research Center assumed the preliminary fault plane in a west-northwest–east-southeast direction toward northeast-dipping ruptures using geological background information, the source location, the focal mechanism, and source rupture process inversion.

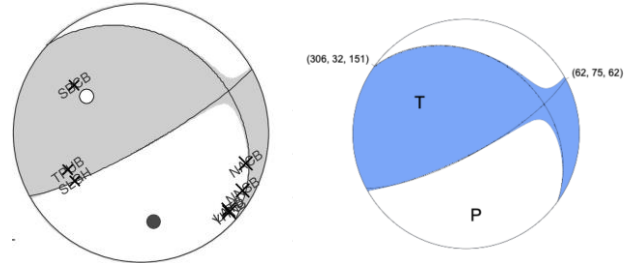


Fig. 3 Focal mechanism announced from the Central Weather Bureau (left) and the United States Geological Survey (right).

The largest peak ground acceleration (PGA) and peak ground velocity (PGV) were observed at approximately 44 gal and 6.0 cm/s, respectively, by referring to the 455 real-time observation stations from the seismic networks operated by CWB and NCREE. Fig. 4 shows ground motion shake maps, including the real-time observations and the new ground motion model of Taiwan, generated using gathered ground motions (Chao et al., 2020). The shake maps provide ground motion information including PGA and PGV, as well as the spectral acceleration at 0.3 s ($Sa_{0.3}$) and 1 s ($Sa_{1.0}$), which can help evaluate the connection between strong ground motions, their cause, and building response.

The high intensity zone exhibiting high PGA, PGV, and $Sa_{1.0}$ in the Taipei basin and Yilan plane could be related to site amplification. The observed dominant frequencies were 1 s and 0.5 to 1 s in the Taipei and Yilan regions, respectively. For instance, the observed response spectrum of a sample station TAP001 in the Taipei basin suggested a main response located at 1 s in north-south direction (Fig. 5) and corresponded to a 1 s dominant frequency calculated from the H/V spectral ratio (HVSR) of weak motions at the same station. Comparing the HVSR from this event and previous weak motions indicate that the site effect from this event behaved as a linear site response prior to and far below design base earthquake (DBE) spectra. In addition, the theoretical radiation pattern calculated from the focal mechanism of this event showed that high ground motion zones were located northwest and southwest from the source, implying that the high intensity zone in the Taipei basin and Yilan plane were superposed through both site amplification and source radiation pattern effects. In contrast, the ground motions on the southwestern side of Taiwan caused by source radiation patterns were not particularly high, probably due to their larger distance from the source.

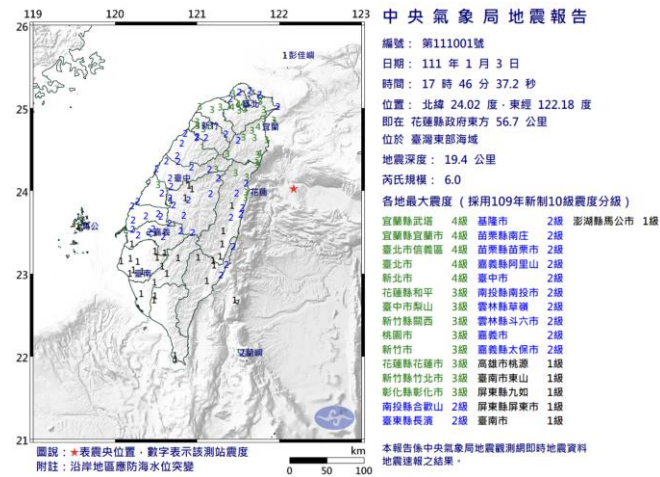


Fig. 1 Event report from January 3 of the M_L 6.0 earthquake occurring at the Hualien offshore.



Fig. 2 A text message sent by the Taiwan Early Seismic Loss Estimation module of the Taiwan Earthquake Loss Estimation System developed by the National Center for Research on Earthquake Engineering (in Chinese).

2 - Evaluation of Seismic Source and Strong Ground Motions

This M_L 6.0 event was resolved as a reverse fault type earthquake accompanied by a strike slip component according to the Taiwan CWB moment tensor solution and the United States Geological Survey (USGS; Fig. 3). The moment magnitude (M_w) was determined to be 6.08 by the CWB and 6.21 by the USGS. The source was located at the upper boundary of the Ryukyu subduction zone. Several large ($M_w > 6.0$) and two huge ($M_w > 7.0$) events have

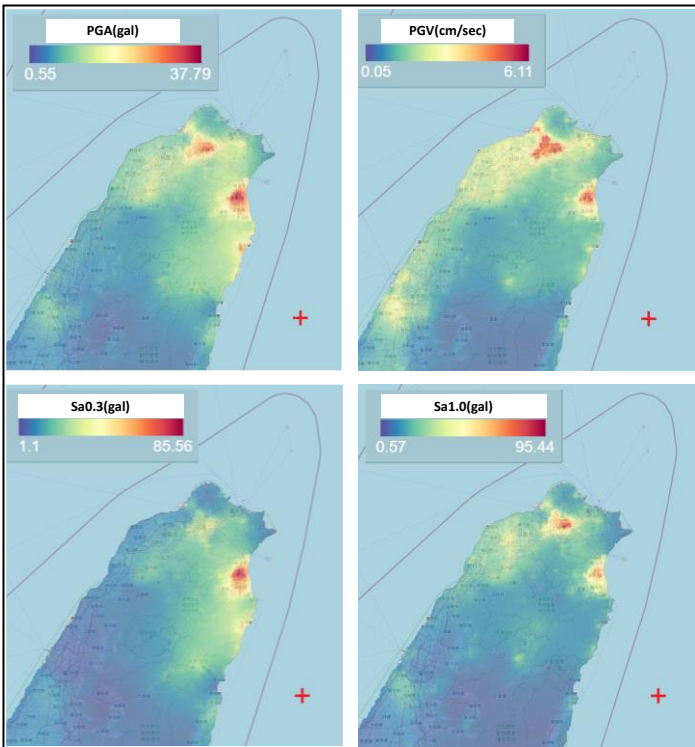


Fig. 4 Shake maps from the real-time National Center for Research on Earthquake Engineering platform for ground motion information, which gathered information from several seismic observation networks, such as CWBSN, TSMIP, SANTA, and EEWS. Upper left: peak ground acceleration (PGA); upper right: peak ground velocity (PGV); lower left: spectral acceleration at 0.3 s (Sa0.3); lower right: spectral acceleration at 1.0 s (Sa1.0).

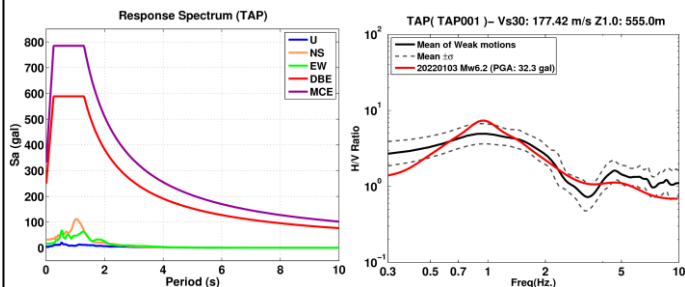


Fig. 5 Observed response spectrum and design spectrum (left) in three components from sample station TAP001, and its site transfer function H/V spectral ratio (HVSr) from shear wave windows (right). The black line indicates the average HVSr of historical weak motions, and could represent the linear site response; the red line represents this event.

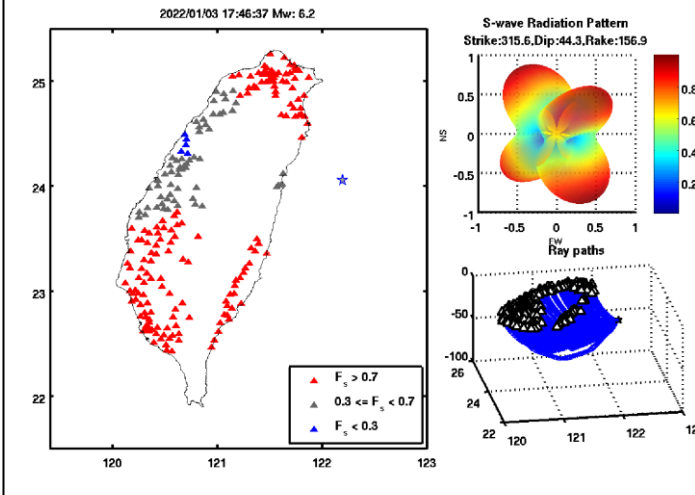


Fig. 6 Theoretical radiation pattern distribution map of TSMIP sites in Taiwan from a pseudo-bending ray-tracing technique using 1D velocity structures. Red, blue, and gray triangles indicate high, low, and intermediate zones, respectively.

3 - Building Strong-Motion Monitoring

The largest intensity generated by the quake reached Level 4, which was measured in Taipei, New Taipei City and Yilan County. The NCREE office building, which is located in the Da'an District of Taipei, measured this seismic intensity level using the strong motion building array measurement record. Using these earthquake duration records as an example, an examination of building dynamic responses to this earthquake was carried out. An extension to the NCREE building was completed at the end of 2020, and comprises the original six-story reinforced concrete structure (B1F to 6F), an added seven-story vertical steel structure (7F to 13F), and a steel service core structure extending from the first floor to the roof on the north side of the building (1F to 13F). The components of the structure are shown in Fig. 7.

After the additions to the NCREE office building, accelerometers were placed on each floor to measure seismic response. During this earthquake, the maximum accelerations measured in the X direction (along Xinhai Road) on 1F, 7F, and the roof floor slabs were 31, 46, and 224 gal, respectively (Fig. 7). A graph of the maximum interstory drift of each floor is shown in Fig. 8. The building remains in an elastic state, and no structural components were damaged. However, after magnifying the dynamic characteristics of the building, the maximum floor acceleration of the roof was 7.2 times that of the first floor. If other buildings exhibit similar amplification effects, there may be considerable impact on auxiliary equipment attached to each floor, including ceiling frames, elevators, and instruments.

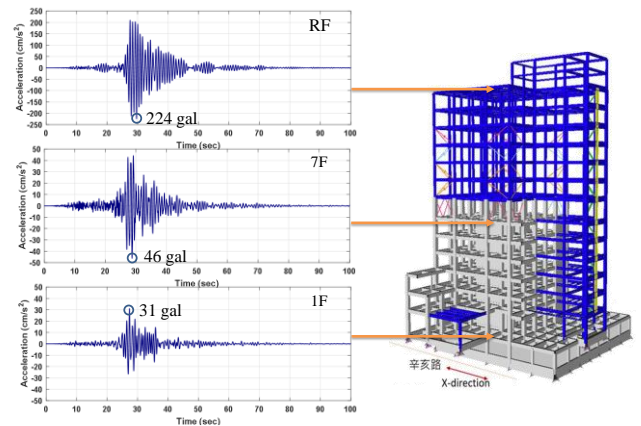


Fig. 7 Earthquake records of the NCREE office building. Grey: RC structure; blue: added steel structure.

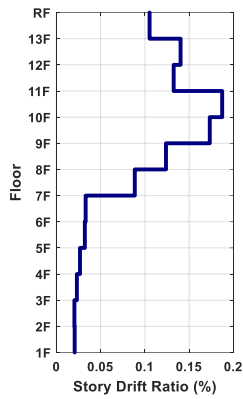


Fig. 8 Maximum interstory drift ratio of the NCREE office building in the X direction.

4 - Bridge Strong Earthquake Monitoring

A total of 15 single-axis and 5 tri-axis acceleration seismometers were installed at the locations shown in Fig. 9. In addition, a newly installed bridge monitoring platform was established and has begun operation (Fig. 10). The NCREE currently maintains the bridge monitoring station, and the recording modes include a period record, seismic event record, and manual user record mode. The current operation of the seismograph allows for obtaining the real-time seismic response of the bridge through seismic data.

The PGA at the bridge site did not reach the earthquake activation threshold (25 gal at magnitude 4) when this earthquake occurred. Therefore, one hour before and one hour after the earthquake excitation, fast Fourier transformations were performed to observe the structural characteristic frequency variation of the bridge and evaluate the bridge status before and after the earthquake.

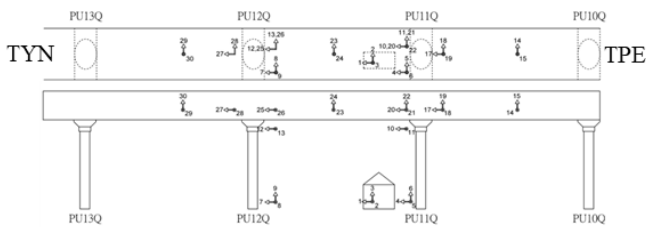


Fig. 9 Sensor configuration of the strong-motion monitoring station TAPBAA.

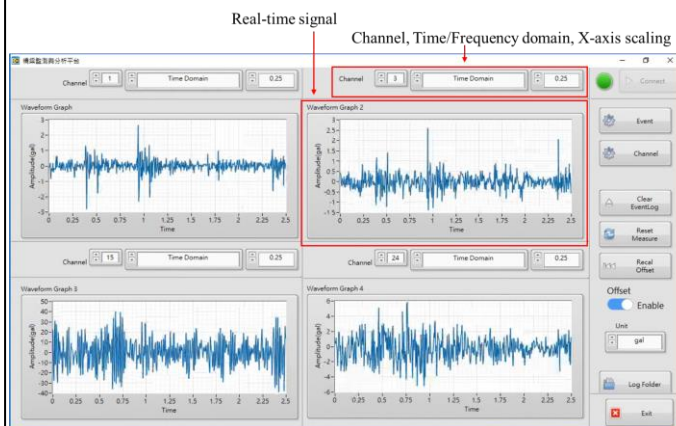


Fig. 10 View of the bridge strong-motion monitoring and analysis platform.

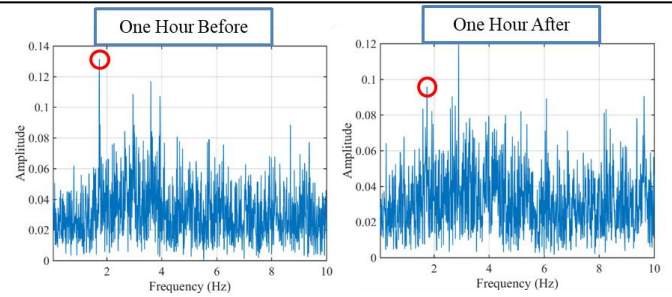


Fig. 11 Bridge frequencies before and after the 2022 01 03 earthquake.

5 - Seismic Damage of Non-Structural Components and Equipment in Buildings

According to the news of the disaster released by electronic media after the earthquake, the significant non-structural seismic damage of commercial buildings in Northern Taiwan can be divided into two categories: damage to elevators and damage to architectural components of buildings. Fortunately, no one was injured from this damage.

Telephone interviews were conducted to gauge the status of the elevator repair cases, and two elevator companies in Northern Taiwan said that the cases could be divided into two categories. The first was that elevator maintenance personnel had to restart the elevators because the earthquake operation procedures were initiated by seismic sensors, which respond to measured magnitudes of four or higher. The other repair category was when cables were disengaged from top pulleys, so that the elevator could not operate and needed to be restored by elevator maintenance personnel, which occurred in a few cases. The elevator repair cases from the two companies were all handled and closed on January 3.

In terms of the seismic damage of architectural components and building contents, components that fell included interior ceiling components, such as many of the glass ornaments of the chandelier system in the banquet hall on the 15th floor of a 16-story commercial building in Wanhua and components of the suspended ceiling system in a large hospital in New Taipei; interior stone veneers of walls built using wet-construction methods, such as those in the elevator waiting area of a large hospital in New Taipei and those in the waiting area at the ground level of the Taipei District Prosecutors Office; and exterior stone veneers from the walls of two Taipei buildings.

Members of Seismic Response Task Team

Chung-Che Chou, Chiun-Lin Wu, Jui-Liang Lin
Kung-Juin Wang, Che-Min Lin, Jyun-Yan Huang
Gee-Jin Yu, Bo-Han Lee, Fan-Ru Lin, Chi-Hao Lin

01/07/2022